

CP40

Cryosat Plus for Oceans

ESA/ESRIN Contract No. 4000106169/12/I-NB

D4.1 Algorithm Theoretical and Validation Document



VERSION 1.0, 4th July 2014

ESA/ESRIN Technical Officer: Jérôme Benveniste

Author Organisation Details


EUROPEAN SPACE AGENCY (ESA) REPORT

CONTRACT REPORT

The work described in this report was done under ESA contract.

Responsibility for the contents resides in the author or organisation that prepared it.

Any copyright statement as necessary


CP40	Algorithm Theoretical and Validation Document	D4.1	
------	---	------	---

AUTHOR/MANAGER/COLLABORATOR LIST

Main Author(s)	Affiliation	Signature
A. Egido	Starlab	
Project Manager	Affiliation	
D. Cotton	SatOC	
Contributors	Affiliation	
M. Caparrini	Starlab	
C. Ray	Starlab	


DISTRIBUTION LIST

Who	Affiliation
D. Cotton	SatOC

CP40	Algorithm Theoretical and Validation Document	D4.1	
------	---	------	---

CHANGE RECORD

ISSUE	DATE	Change Record Notes	Main Author
1	4 th July 2014	First Version	A. Egidio
2			
4			
5			
6			
7			
8			
9			
10			


CP4O	Algorithm Theoretical and Validation Document	D4.1	
------	---	------	---

Abstract

Within the frame of the CryoSat Plus for Ocean (CP4O) ESA project, the SAMOSA-3 fully analytical model, i.e. the current baseline implementation for the Sentinel-3 Level-2 processing, has been updated in order to be able to account for different Level-1 processing approaches. The model updates were focused on the appropriate handling of the energy distribution over the different echoes of the delay-Doppler stack, an application of a Look-Up Table (LUT) for the selection of a variable width Point Target Response (PTR) as a function of SWH, the complete implementation of the SAMOSA-2 model, and an appropriate estimation of the thermal noise from the SAR waveform.


The updated SAMOSA model was integrated within a full waveform retracker, which performs the joint estimation of Sea Surface Height (SSH), Significant Wave Height (SWH), and Sigma₀, by means of an iterative Levenberg-Marquardt minimization algorithm. Within the frame of CP4O, the SAMOSA model was adjusted to the Level-1 processing of the Cryosat Product Prototype (CPP) provided by CNES. The retracker was applied to these data in order to estimate the Level-2 geophysical parameters, which were cross-validated with the SSH, SWH, and Sigma₀ provided in the CPP Level-1b product and calculated by means of a numerical retracker.

The validation of the SAMOSA retracker against CPP was done based on the analysis of a reduced dataset over the North East Atlantic. This comparison showed that the SAMOSA analytical retracker could provide unbiased estimations of SSH, SWH and Sigma₀, with respect to the numerical CPP retracker solution, with very low error standard deviation in all cases.

CP40	Algorithm Theoretical and Validation Document	D4.1	
------	---	------	---


Contents

1	Introduction	9
1.1	Purpose, Scope and Goals	9
1.2	Documents	10
2	Overview	11
3	Algorithm Description	12
3.1	Theoretical Description	12
3.1.1	Physics of the Problem.....	12
3.1.2	Mathematical Description of the Algorithms.....	15
3.2	Scientific Results and Error Analysis	20
4	Assumptions, Constraints, and Limitations	21
4.1	Practical Considerations	21
4.1.1	Input Data.....	21
4.1.2	Ancillary Information	21
4.1.3	Output.....	21
4.2	Programming Considerations	21

CP40	Algorithm Theoretical and Validation Document	D4.1	
------	---	------	---


Figures

Figure 1: Comparison between the optimum fit for the CPP Level-1b SAR waveform (in black), the CNES numerical model (in blue), and the SAMOSA-3 model (in red).	12
Figure 2: (a) SWH estimation with the SAMOSA-3 retracker in comparison with the CNES estimation provided in the CPP product. (b) SSH differences.....	13
Figure 3: CNES CPP SAR Altimeter processing scheme. From [Boy & Moreau, OSTST 2012]..	14
Figure 4: (a) Delay/Doppler Level-1b stack SAMOSA model; (b) trimmed delay/Doppler stack.	16
Figure 5: SAMOSA best fit waveforms after stack trimming for (a) low SWH, and (b) high SWH.	16
Figure 6: Variable PTR width as a function of SWH. In blue circles, LUT provided by Salvatore Dinardo, in red, analytical quadratic formula.	17
Figure 7: SAR-Altimeter waveform leading edge for: (a) low SWH, and (b) high SWH conditions.. In black: CryoSat data; in blue: CPP model; in red: SAMOSA model. Green diamonds show the estimated starting position.....	19
Figure 8:	20

CP40	Algorithm Theoretical and Validation Document	D4.1	
------	---	------	---

Abbreviations and Definitions

CNES	Centre National d'Etudes Spatiales
CP40	Cryosat Plus 4 Oceans
RCMC	Range Cell Migration Correction
SAR	Synthetic Aperture Radar
SIRAL	Synthetic aperture Interferometric Radar ALtimeter
SSH	Sea Surface Height
SSB	Sea State Bias
SLA	Sea Level Anomaly
SST	Sea Surface Temperature
STSE	Support To Science Element
SWH	Significant Wave Height

CP40	Algorithm Theoretical and Validation Document	D4.1	
------	---	------	---

1 Introduction

The “Cryosat Plus for Oceans” (CP4O) project is supported under the ESA Support To Science Element Programme (STSE) and brings together an expert consortium comprising, CLS, DTU Space, isardSAT, NOC, Noveltis, SatOC, Starlab, TU Delft, and the University of Porto. The main objectives of CP4O are:


- to build a sound scientific basis for new scientific and operational applications of Cryosat-2 data over four different areas, which are: open ocean, polar ocean, coastal seas and sea-floor mapping.
- to generate and evaluate new methods and products that will enable the full exploitation of the capabilities of the Cryosat-2 SIRAL altimeter, and extend their application beyond the initial mission objectives.
- to ensure that the scientific return of the Cryosat-2 mission is maximised.

1.1 Purpose, Scope and Goals

This document is the Algorithm Theoretical and Validation Document for the Level-1b data tracking, resulting from the work performed during WP4000 – Product Development and Validation. These plans were initially described in the project proposal [RD.1], and have been updated as necessary following the analysis of user requirements [RD.2] and the analysis of the state of the art [RD.3] which is the other deliverable from WP2000.

More information on the processing schemes and techniques is provided in [RD.3] and more detail on the data sets to be used (for product generation and validation is provided in the data set user manual [RD .4]).

The purpose of this document is to provide a clear description of the developed algorithm, and to demonstrate its validity with a reduced dataset.

CP40	Algorithm Theoretical and Validation Document	D4.1	
------	---	------	---

1.2 Documents

RD.1 Cryosat Plus for Oceans, Technical Proposal, SatOC, DTU Space, isardSAT, NOC, Noveltis, STARLAB, TU Delft, University of Porto and CLS, Response to ESA ITT AO/1-6827/11/I-NB, November 2011


RD.2 Cryosat Plus for Oceans - Scientific Requirements Consolidation (D1.1), STARLAB, NOC, CLS, DTU Space, SatOC, ESA Project Report, March 2013.

RD.3 Cryosat Plus for Oceans – Preliminary Analysis Review (D2.1), TU Delft, CLS, DTU Space, isardSAT, NOC, Noveltis, SatOC, STARLAB, University of Porto, ESA Project Report, May 2013.

RD.4 Cryosat Plus for Oceans – Data Set User Manual (D3.2), isardSAT, SatOC, CLS, DTU Space, NOC, Noveltis, STARLAB, TU Delft, University of Porto, ESA Project Report, May 2013.

RD.5 Cryosat Plus for Oceans, Project Plan v3.1, SatOC, May 2013

RD.6 Cryosat Plus for Oceans, Financial, Administrative and Management Proposal, SatOC, DTU Space, isardSAT, NOC, Noveltis, STARLAB, TU Delft, University of Porto and CLS, Response to ESA ITT AO/1-6827/11/I-NB, November 2011

CP40	Algorithm Theoretical and Validation Document	D4.1	
------	---	------	---

2 Overview

This task concerns the selection of the best algorithm(s) to re-track Cryosat-2 SAR mode waveforms over the Open Ocean and to analyse the performance over different ocean dynamics and Sea State condition.

During the SAMOSA projects Starlab derived a fully analytical expression for the SAR waveforms of a delay-Doppler altimeter. Those were upgraded and implemented by means of a fast computation method by expanding the analytical waveform model in a set of basis functions, which could then be pre-stored in Look-up tables (LUT) for improved computational time.

A retracker was implemented based on a non-linear least square algorithm that relies on a Levenberg-Marquardt minimization method. The objective of this task was to validate the analytical model, and the fast computation approach selected for the waveform retracking algorithm.

The analysis was based on the CPP SAR products provided by CNES. The SAR waveforms were retracked by the multilook waveform model developed within SAMOSA and upgraded within CP40. The full analytical model, and the fast computational model (based on LUT) were used for the retracking of the CPP data. This activity was based on Cryosat-2 SAR data from the North-East Atlantic. The period for the analysis comprises a time span of two weeks from 4th January 2012 until 16th January 2012.

A preliminary statistical comparison was performed with the retracking outputs of the SAR numerical model developed by CNES, provided in the CPP SAR product. This allowed to cross-validate the range and SWH provided in the CPP data. The waveform goodness of fit was compared to the one provided by CNES in the CPP data. A single track within the time period specified above was selected as benchmarking tool for the development of the algorithm. This track covers more than 20 latitude degrees and has a SWH range between 2 and 6+ meters, which was considered representative of a general situation.

3 Algorithm Description

3.1 Theoretical Description

The current section provides the theoretical description of the modifications performed on the SAMOSA model within the frame of WP4000 of the CP40 project. The physics of the problem, and the origin discrepancy of the initial SAMOSA model with respect to the SAR Level-1b waveforms provided in the CPP product are analysed next. The mathematical description of the algorithms is provided in a following sub-section.

3.1.1 Physics of the Problem

In Figure 1, the discrepancies between the original SAMOSA-3 model, [Gommenginger et al., 2012] and the CPP SAR waveforms can be readily observed. The Figure shows an arbitrarily chosen CryoSat-2 SAR Level-1b waveform processed with CPP v.12 (in black), together with the CNES numerical waveform model provided in the CPP product (in blue), and the best fit of the SAMOSA model to the SAR waveform (in red). As can be observed, the SAMOSA-3 model fits relatively well the SAR waveform up to range bin 80, and diverts from the data towards the higher waveform delay gates. In essence, the SAMOSA model has an asymptotic behaviour, whereas CPP data decays to zero.

The other notorious discrepancy of the SAMOSA model with respect to the SAR waveform and CNES numerical model is on the waveform foot, where the SAMOSA model underestimates the data.

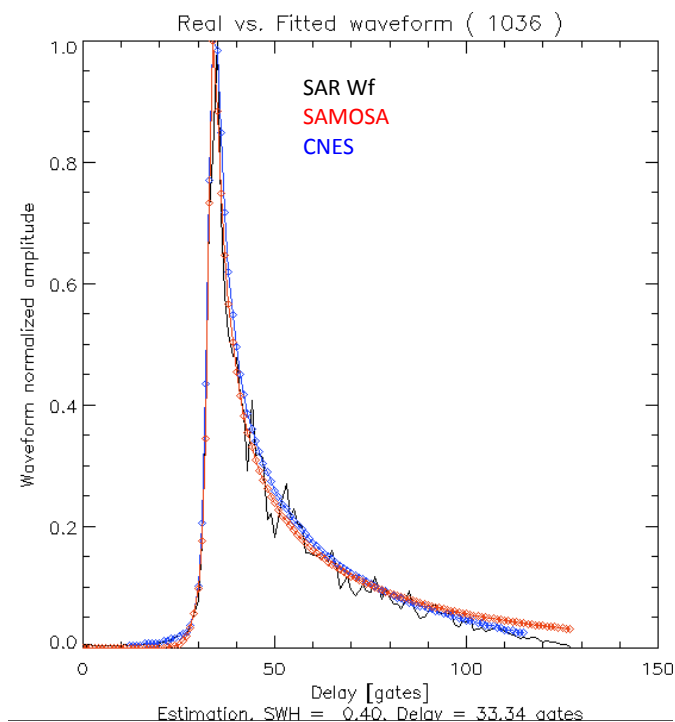


Figure 1: Comparison between the optimum fit for the CPP Level-1b SAR waveform (in black), the CNES numerical model (in blue), and the SAMOSA-3 model (in red).

These discrepancies in the SAMOSA-3 model led to errors in the estimation of the geophysical parameters. For instance, in Figure 2(a) the SWH estimation for a stretch of the benchmarking track is shown. As can be observed, the SAMOSA-3 SWH estimation is biased with respect to CPP by as much as 1 meter. In the same way, the SSH difference between the SAMOSA-3 and CPP retracking outputs, Figure 2(b), shows a decreasing trend which was linked to the increase in SWH.

The cause for the miss-modelling of CPP data was determined to rely mainly on the distribution of the energy over the different Doppler beams of the stack. In the CPP processor, the different Doppler beams of the stack are range cell migrated, in order to correct for their relative range displacement with respect to the zero Doppler beam. This is the so called Range Cell Migration Correction (RCMC). However, the Doppler beams of the Level-1 stack are trimmed to the edge of the correlation window. This has the effect that the range bins out of the limits of the waveform window are set to zero, which leads to a parabolic shape on the range cell migrated stack. This can be observed in Figure 3. When the Doppler beams are multi-looked in a later stage the number of effective looks decreases towards the waveform tail, which makes it to decay to zero.

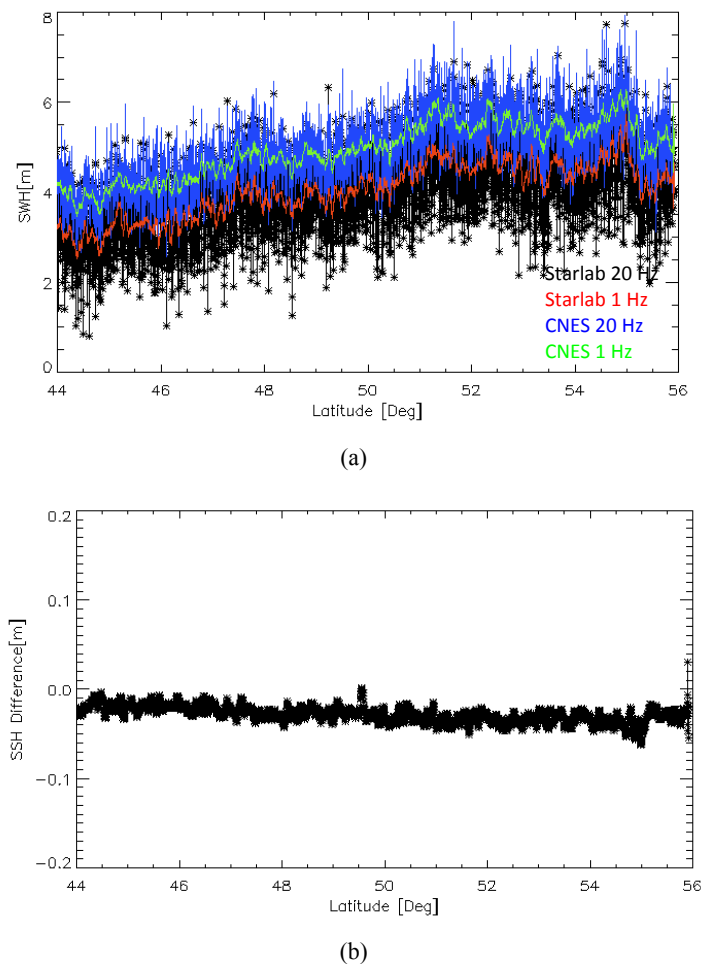


Figure 2: (a) SWH estimation with the SAMOSA-3 retracker in comparison with the CNES estimation provided in the CPP product. (b) SSH differences

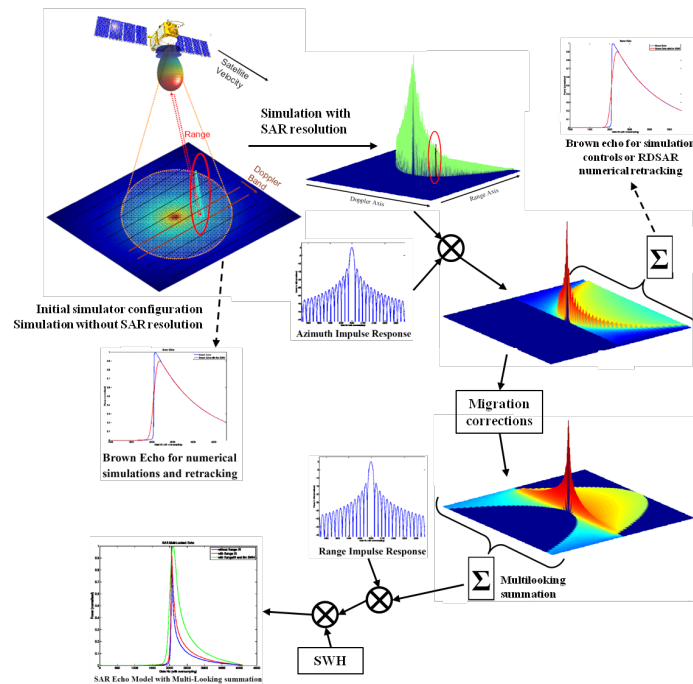


Figure 3: CNES CPP SAR Altimeter processing scheme. From [Boy & Moreau, 2012].

In addition to the previous effect, Salvatore Dinardo determined by comparing the outputs of the numerical CryoSat SAR model and the analytical SAMOSA model, that in order to be able to fit, the Point Target Response (PTR) width of the model needed to have a varying value in order to be able to fit the synthetic waveform generated by the numerical calculation. Despite the fact that the cause of this could not be clearly identified, this effect is linked again with the radar energy distribution over the sea surface, which depends on the sea state; the SAMOSA model assumes a Gaussian PTR for the model, which fits well the SAR altimeter impulse response if the radar echoes are filtered by means of a Hamming window. However, the CPP processor does not include such a windowing function, and therefore the impulse response of the radar is a sinc function, which could lead to discrepancies between the CPP data and the model with a certain dependency on the sea state.

It was also determined during this study that the full SAMOSA model, i.e. the zero (f_0) and first (f_1) order expansion in the skewness of the sea state. In the SAMOSA-3 model, the first order term was neglected for simplicity, justifying this truncation of the model in the fact that the f_1 term is much smaller in magnitude than the f_0 term. However, its effect is more important for high SWH, as observed in [Ray and Martin-Puig, 2012] and verified during this task.

Finally, the thermal noise on the SAR waveforms had to be accounted for in an appropriate way in order to allow for a correct normalization of the waveforms and model. If this is not well considered the net effect is a stretching or widening of the model waveform, which incurs in errors in the estimation of SWH.

All these updates have been implemented in the SAMOSA-3 model. Their mathematical description is provided next.

CP40	Algorithm Theoretical and Validation Document	D4.1	
------	---	------	---

3.1.2 *Mathematical Description of the Algorithms*

As introduced in the previous section, the upgrades of the SAMOSA-3 model were focused on the following four main aspects:

- trimming of the range cell migrated stack,
- Variable PTR width implementation
- Full SAMOSA model implementation
- SAR waveform thermal noise estimation

The mathematical description of these algorithms is reviewed next.

3.1.2.1 Trimming of the range cell migrated stack

As introduced in the previous section, in order to be able to reproduce the CPP data, the SAMOSA stack model needs to be trimmed according to the range cell migration of each of the Doppler beams. The range cell migration of the stack Doppler beams is performed multiplying the each of the stack Doppler beams by the following complex exponential:

$$e^{i2\pi\beta(\alpha x l 2 c h - 2 s x l c) \tau n}$$

where:

- $\beta = BW / \tau p$ Chirp Bandwidth, over pulse duration
- $x l = L x l$ Along-track resolution (Lx) times Doppler beam.
- h Platform height
- s Earth slope
- c Speed of light in vacuum
- τn Range gate n

Considering that the Earth slope equals zero, the number of range gates that need to be range-cell migrated for each Doppler beam can be calculated as:

$$\delta l = \alpha x l 2 2 h L z$$

where Lz is defined as the radar range resolution; $Lz = c / BW$. In the same way, the range gates of the range-cell migrated stack, $P_{k,l}$, that need to be set to zero are specified for the Doppler beam, l , are straightforwardly defined as:

$$P_{k,l} = 0 ; k > 128 - \delta l$$

where k refers to the range gate of the specific Doppler beam. The trimmed stack in comparison with the un-corrected stack can be observed in Figure 4. As can be observed, the characteristic parabolic shape of the Range cell migration can be observed in the trimmed stack.

As mentioned above, this has a remarkable impact on the multi-looking. This effect can be readily appreciated in the SAMOSA-3 output waveforms if compared to the CPP Level-1b data. Figure 5 shows the best fit of the SAMOSA-3 model, including the stack trimming, to the actual CryoSat-2 data. As can be observed, the SAMOSA waveform has a perfect correspondence with both the SAR data, and CNES numerical model.

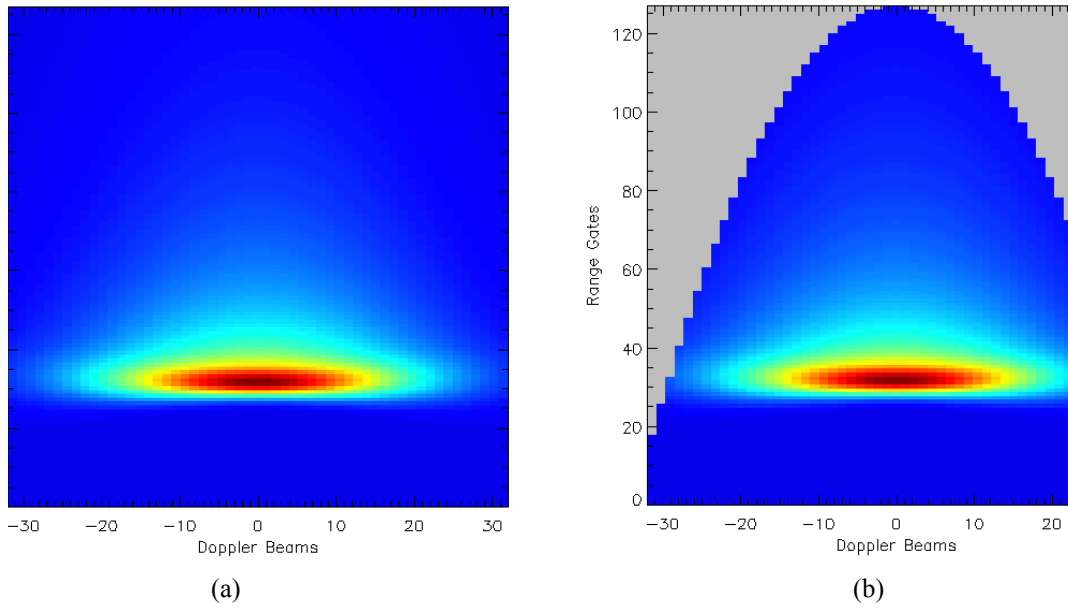


Figure 4: (a) Delay/Doppler Level-1b stack SAMOSA model; (b) trimmed delay/Doppler stack.

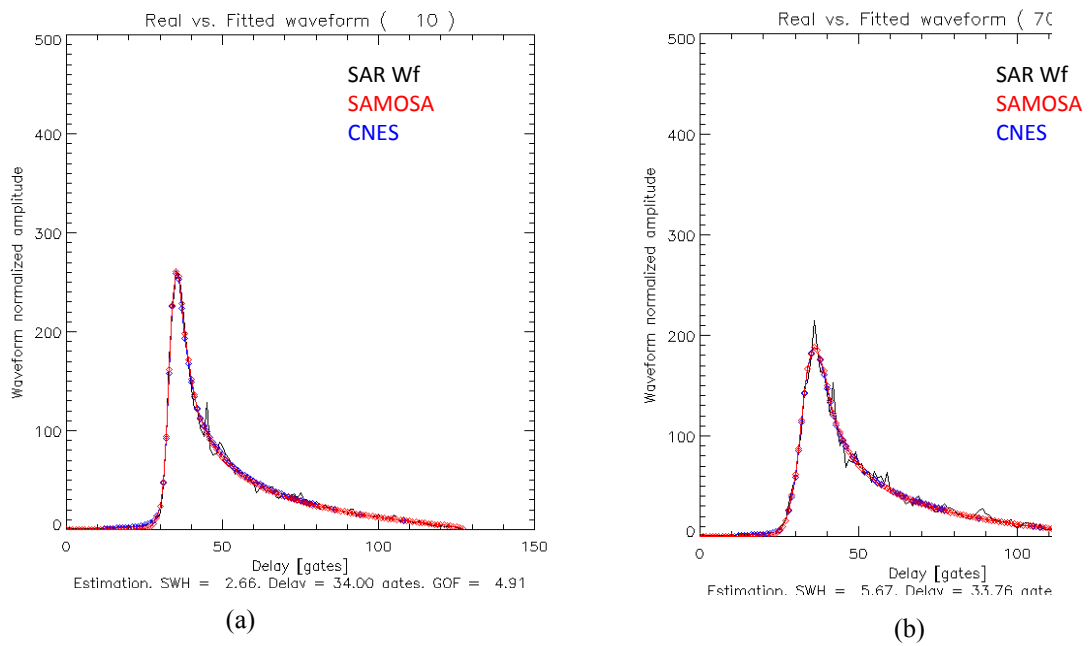


Figure 5: SAMOSA best fit waveforms after stack trimming for (a) low SWH, and (b) high SWH.

3.1.2.2 Implementation of the Variable PTR width

As mentioned before, a variable Point Target Response (PTR) width, αp value in the SAMOSA model, had to be used in order to be able to provide reliable geophysical parameter estimations. The new αp is defined as a function of the Significant Wave Height. The relationship between αp and SWH was obtained by Salvatore Dinardo (SERCO/ESA (ESRIN)) by comparing the output of the SAMOSA full numerical model echoes and the SAMOSA-3 analytical model. The process for determining this relationship is as follows:

- for each SWH value in input (SWH ranging between 0.1 meter and 10 meter) and for a fixed epoch value (zero), the numerical SAMOSA model and the analytical SAMOSA 3 model are generated using exactly the same radar parameter and geometrical configuration.
- the αp table is built finding, for each SWH in input, the αp value providing the best fit, in rms error term, between the SAMOSA numerical model and the SAMOSA 3 analytical model.
- The αp LUT is applied in real time, (i.e. during the re-tracking algorithm execution), extracting, from the table, the αp value corresponding to the SWH value under iteration.

The αp value as a function of SWH is shown in Figure 6. For a straightforward integration with the model, an analytical formula was derived:

$$\alpha p = A + B \cdot SWH - CD^2$$

with:

$$A = 0.4178$$

$$B = 0.0019$$

$$C = 0.9689$$

$$D = 30.6673$$

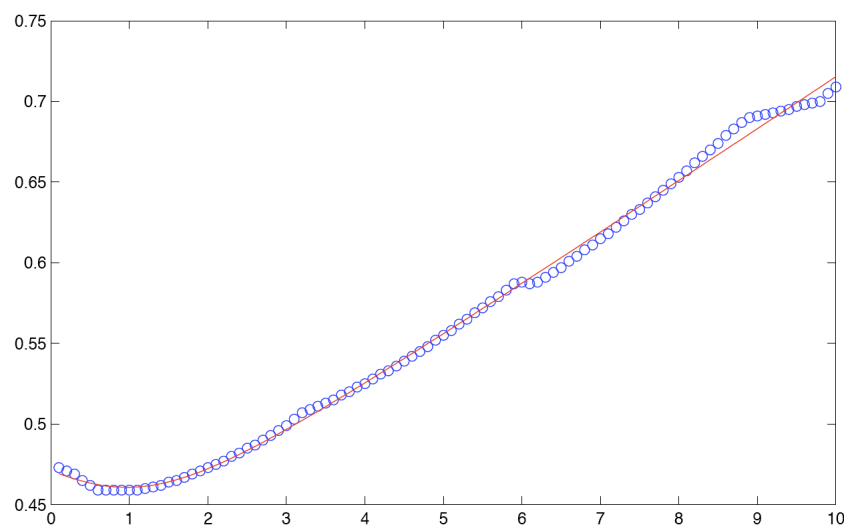


Figure 6: Variable PTR width as a function of SWH. In blue circles, LUT provided by Salvatore Dinardo, in red, analytical quadratic formula.

CP40	Algorithm Theoretical and Validation Document	D4.1	
------	--	------	---

3.1.2.3 Implementation of the full SAMOSA-2 model

As opposed to the SAMOSA-3 model, it was determined during the development of the CP40 project, that the full SAMOSA analytical model, i.e. the so called SAMOSA-2 model had to be implemented in order to be able to provide reliable SWH and SSH estimations. This implies introducing in the model the first order expansion of the sea skewness. The full expression of this model can be found in [Ray, 2011]. Assuming that there is not a slope dependence, and ignoring the mean sea surface and electromagnetic bias, as shown in [Ray and Martin-Puig, 2012], a simplified expression of the this model can be written as:

$$\bar{P}_{k,l} = P_u \sqrt{gl} \Gamma_{k,l}(0) \left\{ f_0(glk) + \frac{\sigma_z}{L_\Gamma} T_k(y_p) gl \sigma_s f_1(glk) \right\}$$

where P_u accounts for all multiplicative factors, f_0 and f_1 are the waveform basis functions as defined in [Ray, 2011], σ_z is the standard deviation of the sea height. The following definition apply also for the previous expression:

$$\Gamma_{k,l}(0) = \exp \left[-\alpha_y y_p^2 - \alpha_x (x_l - x_p)^2 - \alpha_\sigma \alpha_l^2 - (\alpha_y + \alpha_\sigma) y_k^2 \right] \cosh(2\alpha_y y_p y_k)$$

where x_p and y_p are respectively the along- and across- track location of the centre of the beam on the surface, calculated according to the attitude information provided in the CPP product, and

$$x_l = L_x l$$

$$y_k = \begin{cases} L_y \sqrt{k} & \text{if } k > 0 \\ 0 & \text{otherwise} \end{cases}$$

with L_x and L_y the along-track and across-track resolution on the ground. The three scaling constants α_x , α_y , and α_σ are defined as

$$\alpha_x = \frac{8 \ln(2)}{h^2 \theta_x^2} \quad \text{and} \quad \alpha_y = \frac{8 \ln(2)}{h^2 \theta_y^2} \quad \text{and} \quad \alpha_\sigma = \frac{L_c^2}{2\sigma_s^2 h^2}$$

where L_c is the sea correlation length, and θ_x and θ_y the half power beamwidth of the antenna along-track and across-track.

$$T_k(y_p) = \begin{cases} \left(1 + \frac{\alpha_\sigma}{\alpha_y}\right) - \frac{y_p}{L_y \sqrt{k}} \tanh(2\alpha_y y_p L_y \sqrt{k}) & \text{for } k > 0 \\ \left(1 + \frac{\alpha_\sigma}{\alpha_y}\right) - 2\alpha_y y_p^2 & \text{for } k \leq 0 \end{cases}$$

and finally

$$gl = \sqrt{\frac{2\alpha_g}{1 + 4\left(\frac{L_x}{L_y}\right)^4 l^2 + 2\alpha_g \left(\frac{\sigma_s}{L_x}\right)^2}}$$

with $\alpha_g = 12 \alpha_p^2$.

The f_0 and f_1 are the waveform basis functions are implemented by means of Look-Up Tables (LUT) for speeding up their computation.

3.1.2.4 SAR waveform thermal noise estimation

The thermal noise to be added to the SAMOSA model was ultimately estimated from the SAR Level-1b waveforms as the thermal noise estimation provided in the CPP product was not providing reliable results for the estimation of SWH.

An empirical algorithm was developed in order to select the range gates of the SAR waveform from which estimate the thermal noise. The problem with this is that depending on the SWH and the SSH, the position of the first gates of the leading edge can change significantly, which could lead to erroneous estimation of the thermal noise. As can be seen from **Error! Reference source not found.** Figure 7, the position of the leading edge can vary more than 5 range gates between a low and a moderate SWH. Based on the position of the waveform peak, and the mid amplitude of the waveform, the point at which the waveform leading edge starts is calculated as:

$$\begin{aligned} \text{leading_edge_span} &= 2 * (\text{waveform_peak_pos} - \text{half_power_pos}) \\ \text{leading_edge_starting_pos} &= \text{waveform_peak_pos} - \text{leading_edge_span} \end{aligned}$$

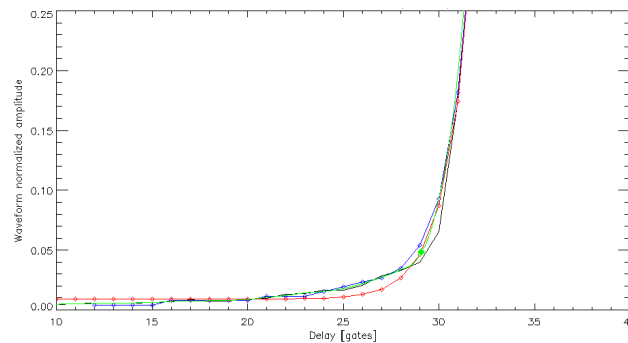
The leading edge starting position is represented with a green diamond in the plots in Figure 7. By an iterative search, the optimal position for the noise calculation was determined to be at

$$\text{noise_calculation_position} = \text{leading_edge_starting_pos} - 9$$

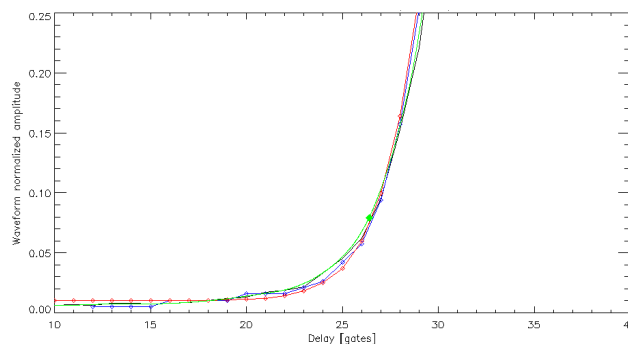
and the noise floor is then calculated as:

$$\text{noise_floor} = \text{mean}(\text{Waveform}[\text{noise_calculation_position}-1 : \text{noise_calculation_position}+1]).$$

With this algorithm, not only the thermal noise is measured, but also the residual energy of the PTR secondary lobes previous to the leading edge. This contributed to an improvement in the estimation of the geophysical parameters.



(a)



(b)

Figure 7: SAR-Altimeter waveform leading edge for: (a) low SWH, and (b) high SWH conditions. In black: CryoSat data; in blue: CPP model; in red: SAMOSA model. Green diamonds show the estimated starting position.

3.2 Scientific Results and Error Analysis

In order to evaluate the retracker performance, a preliminary statistical comparison was performed with the retracking outputs of the SAR numerical model developed by CNES, and provided in the CPP Level-1b product.

A single track was selected as a benchmarking tool for the development of the algorithm. This track covers more than 20 latitude degrees and has a SWH range between 2 and 6+ meters, which was considered representative of a general situation.

The results for the comparison of the SWH and SSH estimations provided by both retracker are shown in Figure 8. Figure 8(a) shows the SWH difference between the updated SAMOSA retracker and the CPP solution. As can be observed, the SWH difference between both solutions is concentrated around zero with no significant slope along the whole track. This is verified if the SWH difference is represented against the CPP SWH estimation, **Error! Reference source not found.**Figure 8 (b). For the 1 Hz product, the SWH mean error and standard deviation yield 3 mm and 3.4 cm, respectively.

In a similar way, the SSH difference against the CPP product is shown in Figure 8 (c-d). A small trend is observed toward increasing SWH values, however this is still below 1 cm for the whole range. The SSH mean error and standard deviation equal 1 mm and 3 mm, respectively.

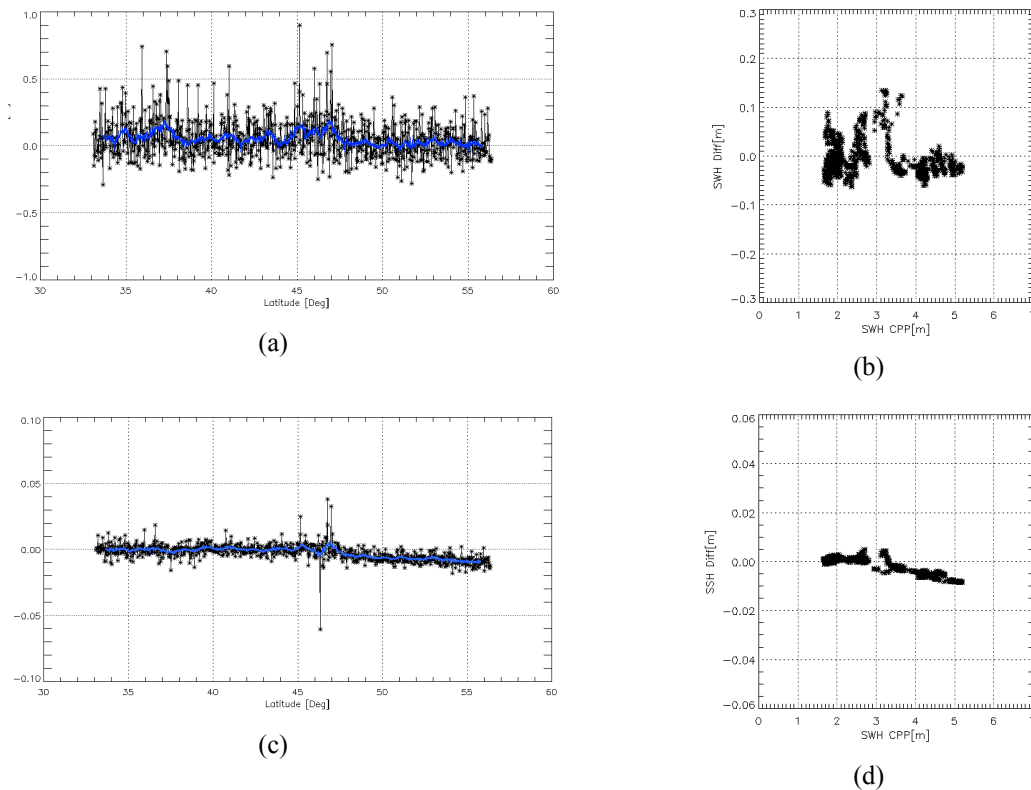



Figure 8: Difference between SAMOSA and CPP retracking solutions: (a) SWH difference along the track; (b) SWH difference vs CPP SWH estimation; (c) SSH difference along the track; (d) SSH difference vs CPP SWH estimation.

CP40	Algorithm Theoretical and Validation Document	D4.1	
------	---	------	---

4 Assumptions, Constraints, and Limitations

4.1 Practical Considerations

4.1.1 Input Data

The data used for this analysis corresponds with two weeks of data over the North East Atlantic, processed by the CNES CPP Level-1b Processor V12.

The CPP L1b Data Products were generated by CNES as from CryoSat-2 SAR FBR (Full Bit Rate) Products (provided by ESA to CNES) after a Delay-Doppler Data Processing on them.

4.1.2 Ancillary Information

Not applicable.

4.1.3 Output

The L2 data products are in netCDF format. One netCDF file was generated for each CPP Level-1b file. The file naming convention is :

[CPP_INPUT_FILENAME].RES.nc

The netCDF format is self-explanatory with all the data field significance described in the attributes. The Goodness of fit (GOF) is calculated as:

$$\text{GOF} = \sqrt{\text{mean}((\text{SAR_Waveform_CPP}[12:116] - \text{Model_Waveform}[12:116])^2)}$$


First and last 12 range bins are discarded for the estimation.

4.2 Programming Considerations

The updated SAMOSA model retracker was implemented in IDL using parallel processing techniques. The implemented code is capable of using all cores available in the machine where it is executed.

The configuration of the retracking is done through a configuration file where the user can select the different configuration parameters that should be set according to the Level-1b input data; i.e. antenna patten, Hamming window, stack trimming, Look-up table, thermal noise estimation, etc. The selected configuration for the production of the Level-2 data is:

- The Reference Time for the TAI Datation is 01/01/2000 00:00:00
- The Reference Ellipsoid is the Topex/Poseidon Ellipsoid
- The SAR Return Power Model is SAMOSA2 with Gaussian PTR approximation corrected by the usage of Look-up Table
- The DDM SAR Power Model masked according to Range-Cell Migrated range bins
- Thermal noise estimation from SAR waveform
- Levenberg-Marquardt Least Mean Squares Minimization Algorithm (LEVLMAR-LSE)
- No static bias has been applied to the range, wave height and sigma nought measurements
- The Doppler Shift Correction has been applied to the range measurements
- The internal path delay has been not applied to the range measurements

CP40	Algorithm Theoretical and Validation Document	D4.1	
------	---	------	---

5 References

- [Boy & Moreau, 2012]: François Boy, Thomas Moreau, et al, “*CryoSat Processing Prototype, LRM and SAR Processing on CNES Side*”, OSTST Venice 2012
- [Gommenginger et al., 2012]: C. Gommenginger, C. Martin-Puig , M. Srokosz, M. Caparrini, S. Dinardo, and B. Lucas, “*Detailed Processing Model of the Sentinel-3 SRAL SAR altimeter ocean waveform retracker*”, SAMOSA3 WP2300 technical Note, ESRIN Contract No. 20698/07/I-LG "Development of SAR Altimetry Mode Studies and Applications over Ocean, Coastal Zones and Inland Water", Version 2.1.0, 16 March 2012, 75 pages.
- [Ray and Martin-Puig, 2012]: C. Ray and C. Martin-Puig, “*SAMOSA models trade-off technical note*”, D1, SAMOSA3-CCN2, February 2012.
- [Ray, 2011]: C. Ray, “*Further Development of SAR Altimeter Waveform model*”, D8, SAMOSA-CCN, August 2011.